Int. J. Heat Mass Transfer. Vol. 36, No. 7, pp. 1981–1991, 1993
Printed in Great Britain

0017–9310/93 $6.00+0.00
Pergamon Press Ltd

Modelling of the effect of turbulent two-phase flow friction decrease under the influence of dispersed phase elements

L. V. ZAKHAROV, A. A. OVCHINNIKOV and N. A. NIKOLAYEV
Mechanical Faculty, Kazan Institute of Chemical Engineering, Kazan, 420015, Russia

(*Received* 25 *May* 1989 *and in final form* 5 *January* 1990)

Abstract—Consideration is given to the problem concerning the interaction of a continuous turbulent flow with a dispersed impurity uniformly distributed in it with the account of the involvement of particles into energy-intensive fluctuations of the continuous medium. Correlations are obtained relating the drag reduction in the turbulent two-phase flow to the size of particles and dispersed phase concentration. The limitations are established which should be imposed on the concentration and size of particles to attain the regime of reduced drag in a two-phase turbulent flow. The theoretical relations obtained are in good agreement with the available experimental results.

1. INTRODUCTION

THE JOINT motion of a carrying turbulent flow and of the dispersed impurity distributed in it in the form of solid particles, gas bubbles or liquid drops forms a basis for many processes taking place in the most variegated (in both function and design) apparatus of chemical technology. In view of this, considerable effort has been devoted recently to the study of the mutual effect of the moving phases and to the influence of dispersed phase on the intensity of transfer processes in a continuous flow. The analysis of the available work pertaining to this subject showed that two-phase turbulent flows possess a number of distinguishing features which are not characteristic of single-phase flows [1–15].

The experimental results listed in Table 1 allow it to be concluded that a small number of particles of a certain size present in a turbulent flow leads to the effect of turbulent flow 'laminarization' characteristic of which is the reduction of drag due to the dispersed phase-induced reconstruction of the macro- and microstructure of flow. This offers a practical opportunity to control the carrying flow parameters through the action of particles on the continuous medium for enhancing the positive effect. This control should be based on relations that connect the kinematic characteristics of flow with the dimensions and concentration of the dispersed phase suspended in it. In view of this, the object of this study was to establish the law that would govern the effect of friction reduction in a turbulent two-phase flow and to give its mathematical description.

2. ANALYSIS OF FAMILIAR EXPERIMENTS

In order to obtain definite knowledge about the influence of particles on the energy losses by a turbulent two-phase flow and also to evaluate the intensity of the affecting factors, the classification of the available experimental material was carried out on the following principles.

(i) Orientation of the test section in space (the influence of body forces).

(ii) Characteristics of the continuous medium (liquid or gas) and of the transport velocity.

(iii) Dimensions and concentration of the dispersed phase.

The experiments with air–solid particle systems in horizontal tubes carried out by Dogin [1], Mulgi [2], Yotaki and Tomita [3], Laats [4], Pechenegov [5], and by a number of other researchers [6–10] covered fairly large ranges of the mean mixture velocities, particle sizes and of the test pipeline diameters. The value of mass concentration of particles varied in the experiments from fractions of a kilogramme to 10–15 kg of particles per kilogramme of air.

The results of these works, presented in Table 1 and summarized in Fig. 1(a), testify to the possibility of both increasing the drag of a turbulent two-phase flow [1–6, 8] and decreasing it appreciably under certain conditions [4, 7, 9, 10] which include a low mass concentration of dispersed phase and also a small size of particles (in the majority of experiments the reduction of friction was observed in the presence of particles as small as 15–30 μm). The size of particles that allows the effect of drag reduction in horizontal tubes to be seen grows with the channel diameter and decreases with an increasing density of dispersed phase.

The trends noted are also observed in other experimental systems (water–solid particles [11]) and in vertical and inclined pipelines ([4, 9, 10, 12–15], Fig. 1(b)).

The experimental data taken from the relevant

NOMENCLATURE

c	volumetric concentration of dispersed phase
$\bar{c}$	averaged field of volumetric concentration
c', c''	macro- and microscale fluctuations of concentration
C_2	coefficient of averaged sliding of phases
D	diameter of channel
D_{tr}	coefficient of turbulent diffusion of particles
d_p	diameter of particles
g	free fall acceleration
p	instantaneous pressure
$\bar{p}$	averaged component of instantaneous pressure
p', p''	total pressure components, inherent in macro- and microscale vortices
R	radius of channel
Re	channel diameter-based Reynolds number
u_i	instantaneous velocity of continuous medium
$\bar{u}_i$	averaged component of instantaneous velocity of continuous medium
u_m	mean velocity of continuous medium
u', u_i''	fluctuation components of macro- and microscale instantaneous velocity
$\bar{u}_+$	dimensionless averaged velocity of continuous medium
u_*	dynamic velocity
v_i	instantaneous velocity of particle
$\bar{v}_i$	averaged component of instantaneous particle velocity
v_i'	fluctuational velocity of particle
V	certain volume
$x_{i,l}$	coordinate
y_+	dimensionless distance from the wall.

Greek symbols

δ_L	viscous sublayer thickness
δ_+	dimensionless viscous sublayer thickness
λ_1, λ_2	coefficient of hydraulic resistance of single- and two-phase flows
μ_p	degree of involvement of particles in fluctuational motion
ρ, ρ_p	density of continuous medium and particles
τ	time of relaxation of particles
τ_w	shear stress on the wall
ν, ν_T	kinematic and turbulent kinematic viscosities.

literature and classified by the similarity of a number of certain symptoms thus showed the double influence of dispersed phase on the magnitude of energy losses by a two-phase flow. On the one hand, this is the growth of losses in the case of large particles and their concentration in the flow, on the other hand, this is the reduction in energy losses in a two-phase flow as against a one-phase flow in the presence of small particles in the flow and their small concentration. The increase in the concentration of particles leads to the loss of the effect of friction reduction and to the growth of the drag of a two-phase flow.

Of particular practical interest are those experimental data which indicate the possibility for reducing the drag of a two-phase flow in comparison with that of a single-phase flow under certain conditions.

The results of works [4, 7–10] obtained with horizontal orientation of the test section and use of small particles of different diameters revealed their critical size when the influence of the dispersed phase on the drag vanishes (Figs. 2(a) and (b)). Determination of the critical size of particles in a vertically ascending flow from the data of refs. [4, 10, 14] is presented in Fig. 2(c).

Comparison of Figs. 2(a), (b) and (c) and their analysis allowed the confirmation of the following regularities.

(i) An increase in the dimensions of the channel leads to the growth of the upper critical size of particles.

(ii) An increase in the density ratio of the phases lowers this limit.

(iii) The critical dimensions of the horizontal and vertical orientations of the flow differ substantially from one another.

Moreover, the behaviour of the relations in Figs. 2(a), (b) and (c) indicates the presence of the minimum and maximum sizes of particles of the dispersed phase in the range between which the drag reduction effect is manifested.

The earlier theoretical constructions [16–18] showed that the mathematical description of the drag reduction effect can be obtained on the basis of Kolmogorov's ideas about the turbulent two-phase flow pulsational energy balance.

It is known that in single-phase turbulent flows the drag is related to the kinematic parameters as

$$\lambda_1 = 8\tau\omega/\rho U^2 m \tag{1}$$

$$\tau_w = (11.5\nu/\delta_L)^2\rho. \tag{2}$$

Relations (1) and (2) show that the value of hydraulic losses, just as the value of shear stresses at the wall, is uniquely connected with the thickness of

Table 1. The results of experimental investigations of turbulent two-phase flows

References 1	Dimension (diameter) of a channel D (mm) 2	Material and sizes of particles, d_p (mm) 3	Density of particles, r_p (kg m^{-3}) 4	Interval (range) Re 5	Range variation of concentration of S (kg kg^{-1}) 6	Number of the curve in Figs. 1a,b 7	λ_2/λ_1 8
	Horizontal tubes with air as a continuous medium						
[1]	125.0	millet, 1900	1332	12 000–3001 000	0–4	—	>1
[2]	26.0	bronze, 35	8500	52 000–87 000	0–14	—	>1
[3]	130.8	soy beans, 5600	1250	70 000–120 000	0–10	—	>1
[4]	12.7	glass, 97	2500	25 400	0–3	—	>1
[4]	32.7	glass, 40	2500	40 000	0–2	1	>1
[4]	32.7	corundum, 17	3970	40 400	0–1.5	2	0.85
	Vertical tubes with air as a continuous medium						
[4]	22.2	glass, 10	2500	25 000	0–1.5	12	0.64
[4]	22.2	glass, 20	2500	24 420	0–1.5	13	0.5
[4]	22.2	glass, 34	2500	23 680	0–1.5	14	0.3
[4]	22.2	glass, 59	2500	23 680	0–1.5	15	0.37
[4]	25.4	glass, 250	2500	28 800	0–1.5	16	1.3
	Horizontal tubes with air as a continuous medium						
[5]	14.0	marble, 110	2600	6500–25 000	0–4	—	>1
[6]	24.4	boron carbide, 4.65	—	3720–6460	300–400	—	>1
[7]	32.7	electrocorundum, 15	3970	40 400–62 000	0–3	3	0.6
[7]	32.7	electrocorundum, 23	3970	40 400–62 000	0–3	4	0.7
[8]	31.8	glass, 170	2500	25 000–100 000	1–6	5	>1
[8]	31.8	glass, 340	2500	25 000–100 000	1–5	6	>1
[8]	31.8	glass, 570	2500	25 000–100 000	1–6	7	>1
[9]	22.1	glass, 15	2500	11 000–23 000	0–1	8	0.9
[9]	22.1	glass, 36	2500	11 000–23 000	0–1	9	>1
[9]	22.1	glass, 55	2500	11 000–23 000	0–1	10	>1
[10]	22.1	glass, 21	2500	11 000–23 000	0–1	11	0.9
[10]	22.1	glass, 21.6	2500	11 000–23 000	0–1	—	0.89
	Vertical tubes with air as a continuous medium						
[10]	22.1	glass, 15	2500	11 000–23 000	0–1	17	0.9
[10]	22.1	glass, 21	2500	11 000–23 000	0–1	—	0.88
[10]	22.1	glass, 21.6	2500	11 000–23 000	0–1	18	0.86
[10]	22.1	glass, 36	2500	10 000–15 000	0–2	19	0.7
	Horizontal rectangular channel with air as a continuous medium						
[11]	40*40	polystyrene, 320	—	11 580–13 000	0–0.44%	—	<1
	Vertical tubes with air as a continuous medium						
[12]	50.0	anionite, 520	1130	29 700–66 700	0–2	—	<1
[13]	76.2	zinc, 40	7150	35 000	0–3	—	0.9
[14]	25.4	aluminium, 15	2700	100 000–180 000	0–6	20	0.6
[14]	25.4	aluminium, 40	2700	100 000–180 000	0–5	21	0.65
[14]	25.4	aluminium, 70	2700	100 000–180 000	0–5	—	0.68
	Vertical tubes with water as a continuous medium						
[15]	24.0	rubber, 922	1200	3000–40 000	0–1%	—	0.85

the viscous sublayer. In turn, the viscous sublayer thickness in a turbulent flow is governed by the local balance of the production and dissipation. According to Barenblatt [16], the mechanism underlying the turbulent friction reduction is determined by an additional dissipation of turbulent energy expended for suspending particles in the gravity field. An alternative viewpoint attributes the drag reduction effect to the aerodynamic interaction of phases and selective quenching of a portion of the energy spectrum, which corresponds to large wave numbers [17], or to the distortion of a portion of the energy spectrum, which corresponds to small wave numbers [18].

Comparison of different views on the problem with the above analysis of familiar experimental results dictates the necessity of simultaneous consideration of the aerodynamic interaction of phases and interaction of particles with the fields of body forces when constructing the mathematical description of the phenomenon.

3. MODEL

The mathematical description of the effect of drag reduction is based on the momentum transfer equations for continuous and disperse media, written for

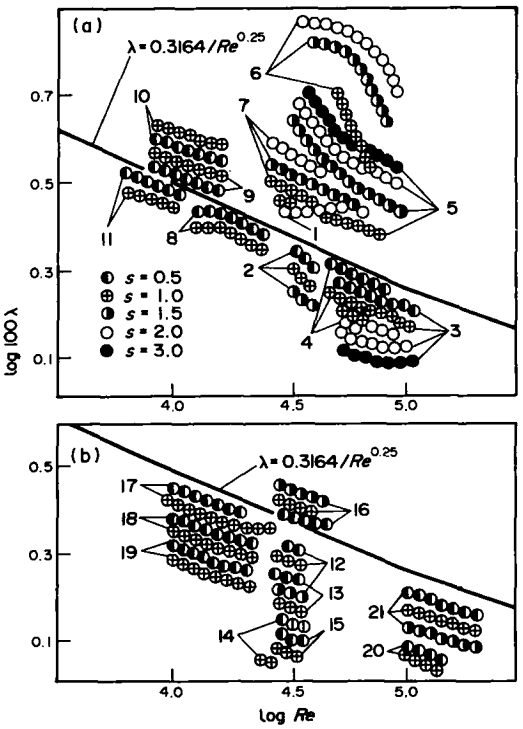

FIG. 1. The summarized results concerning the dispersed phase effect on the friction drag of a turbulent two-phase flow. (a) horizontal tubes; (b) vertical tubes.

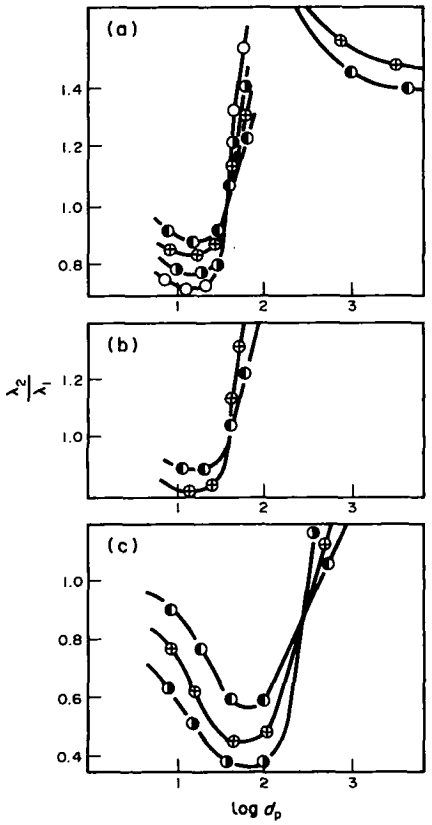

FIG. 2. Critical dimensions of particles. (a) $Re = 40\,400$, 31.8 mm $\leqslant D \leqslant$ 32.7 mm, horizontal tube; $d_{p\,cr} \approx 31$ μm; (b) $Re = 20\,000$, $D = 21.1$ mm, horizontal tube, $d_{p\,cr} \approx 28$ μm; (c) $Re = 25\,000$, $DS = 22.2$ mm, vertical tube, $d_{p\,cr} = 165$ μm. Symbols as in Fig. 1.

instantaneous velocities and modified with allowance for their two-phase nature, and on the continuity equation for a continuous medium

$$\frac{\partial u_i}{\partial t} + u_e \frac{\partial u_i}{\partial x_e} = -\frac{1}{\rho}\frac{\partial p}{\partial x_i} + \nu \frac{\partial^2 u_i}{\partial x_e \partial x_e} - g_i - c\frac{\rho_p}{\rho}\frac{1}{\tau}(u_i - v_i) \quad (3)$$

$$\frac{\partial v_i}{\partial t} + v_e \frac{\partial v_i}{\partial x_e} = \frac{1}{\tau}(u_i - v_i) - g_i \quad (4)$$

$$\frac{\partial u_i}{\partial x_i} = 0. \quad (5)$$

The entire spectrum of fluctuations is divided into two main intervals: the interval of low frequencies where the extraction of energy from the averaged flow or the 'production of turbulence' take place and the interval of mean and high frequencies for which the characteristic feature is the transfer of energy over the spectrum and its dissipation into heat. The instantaneous velocity of the turbulent flow was, therefore, represented as a sum of the averaged velocity and two pulsational components corresponding to turbulent vortices of macro- and microscales [19]

$$u_i = \bar{u}_i + u_i' + u_i''. \quad (6)$$

It must be borne in mind that the following condition is valid for developed turbulent flows

$$\bar{u}_i \gg u_i' > u_i''. \quad (7)$$

Since the low-frequency macroscale formations are responsible for the 'production of turbulence', the increase in the local energy dissipation in a turbulent two-phase flow is governed by the interaction of particles of the dispersed phase with precisely this energy-intensive portion of the spectrum.

Assume that the flow contains a dispersed phase consisting of identically sized particles with small volumetric concentration and that the aerodynamic interaction of phases obeys the Stokes law, as is already incorporated in the original system of equations (3)–(5). The distribution of the dispersed phase over the flow cross-section is uniform. With particles being rather small (the condition for the applicability of the Stokes law), it is possible to assume a close enough coincidence between the motion of each particle and that of the liquid itself if it had occupied the same volume as the particle does. Consequently, the concentration of the dispersed phase can be represented by

$$c = \bar{c} + c' + c''. \quad (8)$$

The connection between the averaged and fluctuational velocities of the flow and of the particles is

described by relations involving phase slip coefficients

$$\mu_p = v_i'/(u_i'+u_i'') = (1+u_*\tau/0.1R)^{-1/2} \quad (9)$$

$$C_2 = \bar{v}_i/\bar{u}_i. \quad (10)$$

In order to determine the degree of the involvement of particles in the pulsational motion of the stream, Mednikov's formula [20] was used. Up until now, no single correlation has been obtained for determining the coefficient of the averaged slip of phases C_2. It is only safe to say that the mean-integral lag of particles behind the continuous medium amounts to 5–10%. Based on experimental investigations, a number of authors obtained empirical and semi-empirical expressions for determining C_2 which have a very limited application, but which can, however, be employed in calculations when the parameters of the systems coincide with, or are close to, the experimental conditions. The list of these formulae is given in ref. [20].

With the concentration and the size of the dispersed phase being small, the transition was made to the description of the two-phase system by equations for a continuous medium with source terms. In this case a new term appears on the RHS of equation (3) for a certain acceleration of the continuous medium due to the interaction of the dispersed phase with the gravitational field

$$-g_i\rho_p V_p = \rho V a \quad \text{or} \quad a = -g_i\frac{\rho_p}{\rho}c \quad (11)$$

$$\frac{\partial u_i}{\partial t}+u_e\frac{\partial u_i}{\partial x_e} = -\frac{1}{\rho}\frac{\partial p}{\partial x_i}+\nu\frac{\partial^2 u_i}{\partial x_e\,\partial x_e} - g_i - c\frac{\rho_p}{\rho}\frac{1}{\tau}(u_i-v_i) - g_i\frac{\rho_p}{\rho}c. \quad (12)$$

With allowance for the connections introduced, the equations for the instantaneous velocities and averaged flow parameters were reduced to the form

$$\frac{\partial \bar{u}_i}{\partial t}+\frac{\partial}{\partial t}(u_i'+u_i'')+\frac{\partial}{\partial x_e}(\bar{u}_e u_i''+u_e''\bar{u}_i)+\frac{\partial(\bar{u}_i\bar{u}_e)}{\partial x_e} + u_e'\frac{\partial \bar{u}_i}{\partial x_e}+\bar{u}_e\frac{\partial u_i'}{\partial x_e}+\frac{\partial}{\partial x_e}[(u_i'+u_i'')(u_e'+u_e'')] = -\frac{1}{\rho}\frac{\partial}{\partial x_i}(\bar{p}+p'+p'')+\nu\frac{\partial^2}{\partial x_e\,\partial x_e}(\bar{u}_i+u_i'+u_i'')\frac{\rho_p}{\rho}\frac{1}{\tau} \times\{(1-c_2)\bar{c}\bar{u}+(1-\mu_p)\bar{c}(u_i'+u_i'')+(1-c_2)\bar{u}_i(c'+c'') +(1-\mu_p)[(u_i'+u_i'')(c'+c'')]\} - g_i\left(1+\frac{\rho_p}{\rho}(\bar{c}+c'+c'')\right) \quad (13)$$

$$\frac{\partial \bar{u}_i}{\partial t}+\frac{\partial(\bar{u}_i\bar{u}_e)}{\partial x_e}+\frac{\partial}{\partial x_e}[\overline{(u_i'+u_i'')(u_e'+u_e'')}] = -\frac{1}{\rho}\frac{\partial \bar{p}}{\partial x_i}+\nu\frac{\partial^2\bar{u}_i}{\partial x_e\,\partial x_e}-\frac{\rho_p}{\rho}\frac{1}{\tau}\{(1-c_2)\bar{c}\bar{u}_i+(1-\mu_p) \times[\overline{(u_i'+u_i'')(c'+c'')}]\}-g_i\left(1+\frac{\rho_p}{\rho}\bar{c}\right). \quad (14)$$

Traditional transformations of momentum transfer equations (13) and (14) gave the turbulent pulsational energy conservation equation

$$\int\frac{d}{dt}(\tfrac{1}{2}u_i'u_i')\,dV+\int u_i'\frac{\partial u_i'}{\partial t}dV+\int u_i'\frac{\partial}{\partial x_e} \times[(u_i'+u_i'')(u_e'+u_e'')-\overline{(u_i'+u_i'')(u_e'+u_e'')}]\,dV +\int u_i'u_e'\frac{\partial \bar{u}_i}{\partial x_e}dV+\int u_i'\frac{\partial}{\partial x_e}(u_i''\bar{u}_e+u_e''\bar{u}_i)\,dV = -\int\frac{u_i'}{\rho}\frac{\partial}{\partial x_i}(p'+p'')\,dV+\nu\int u_i'\frac{\partial^2 u_i'}{\partial x_e\,\partial x_e}dV +\nu\int u_i'\frac{\partial^2 u_i''}{\partial x_e\,\partial x_e}dV-\frac{\rho_p}{\rho}\frac{1}{\tau}\int\{(1-\mu_p)c\bar{u}_i'(u_i'+u_i'') +(1-c_2)\bar{u}_iu_i'(c'+c'')+(1-\mu_p)u_i'[(u'+u_i'')(c'+c'') -\overline{(u_i'+u_i'')(c'+c'')}]\}\,dV-g_i\frac{\rho_p}{\rho}\int u_i'(c'+c'')\,dV. \quad (15)$$

It is seen from this equation that the fluctuations of concentration and the averaged slip of phases become essential only when the body forces are taken into account.

The analysis of equation (15) in its general form is rather difficult; therefore, a number of complementary conditions were incorporated that reflect the specificity of the flow considered. With allowance for the scale ratio of the instantaneous velocity components, equation (7), the components of the energy balance equation that incorporate the contribution of the microscale fluctuations into the overall balance of fluctuational energy were neglected without evaluating the values of the first and second velocity derivatives; this rather corresponds to the monochromatic representation of the energy intensive portion of the spectrum. The terms of the equation that involved the derivatives of pressure gradient connected with the small scale velocity gradients were also ignored due to their smallness.

With the use of the assumptions adopted and of the energy equilibrium hypothesis for macroscale vortices [19], equation (15) yielded the fluctuational energy balance equation for macroscale vortical structures

$$-\int u_i'u_e'\frac{\partial \bar{u}_i}{\partial x_e}dV = \int u_i'\frac{\partial}{\partial x_e}(u_i'u_e'-\overline{u_i'u_e'})\,dV +\nu\int\left(\frac{\partial u_i'}{\partial x_e}\right)^2 dV+\frac{\rho_p}{\rho}\frac{1}{\tau}\int(1-\mu_p)\bar{c}u_i'u_i'\,dV +\frac{\rho_p}{\rho}\frac{1}{\tau}\int(1-c_2)\bar{u}_iu_i'c'\,dV+\frac{\rho_p}{\rho}\frac{1}{\tau} \times\int(1-\mu_p)u_i'(u_i'c'-\overline{u_i'c'})\,dV+g_i\frac{\rho_p}{\rho}\int c'u_i'\,dV. \quad (16)$$

The left-hand side of this equation determines the rate of energy extraction from the averaged motion.

The first term on the right-hand side of this equation stands for the work done by large vortices to resist additional Reynolds stresses originating due to the presence of these vortices. It can be expressed in terms of the turbulent viscosity and strain rate tensor at the diagonal elements being equal to zero

$$u_i'u_e' - \overline{u_i'u_e'} = -2\nu_T \frac{1}{2}\left(\frac{\partial u_i'}{\partial x_e} + \frac{\partial u_e'}{\partial x_i}\right). \quad (17)$$

The second term on the RHS of this equation gives energy dissipation due to viscosity, the third term takes into account energy dissipation due to the involvement of particles into the pulsational motion of the continuous medium and the fourth term accounts for the dissipation due to the averaged slip of phases. The sixth term corresponds to the flow energy losses to suspend particles in the fields of body forces.

The fifth term represents the work done by large vortices to transfer the mass involved in their motion and, by analogy with equation (17), can be expressed in terms of the turbulent diffusion and concentration fluctuation tensor at the diagonal elements being equal to zero

$$u_i'c' - \overline{u_i'c'} = -2D_{tr} \frac{1}{2}\left(\frac{\partial c'}{\partial x_e} + \frac{\partial c'}{\partial x_i}\right). \quad (18)$$

The fluctuational energy balance equation (16) thus shows that addition to the viscous dissipation, the dispersed phase-carrying turbulent flow also has the mechanism of additional dissipation of turbulent energy which is based on the entrainment of particles into the pulsational motion, averaged slip of phases, pulsational mass transfer and on the loss of energy to suspend the particles.

For small-size particles, it is reasonable to assume the identity between the motions of the dispersed phase particles and of the continuous medium. With allowance for the degree of the entrainment of particles, this made it possible to express the fluctuations of concentration as

$$c'/\bar{c} = \mu_p(u_{i1e}'/\bar{u}_1). \quad (19)$$

Equation (18) involves the coefficient of turbulent diffusion of particles D_{tr}. It was determined from the results of [20] in conformity with Reynold's analogy between the transfer of mass and momentum

$$D_{tr} = \mu_p^2 D_T = \mu_p^2 \nu_T. \quad (20)$$

After the substitution of equations (17)–(20), equation (16) transforms to

$$-\int u_i'u_e' \frac{\partial \bar{u}_i}{\partial x_e} dV = \int u_i' \frac{\partial}{\partial x_e}\left[-2\nu_T \frac{1}{2}\left(\frac{\partial u_i'}{\partial x_e} + \frac{\partial u_e'}{\partial x_i}\right)\right] dV$$

$$+\nu \int \left(\frac{\partial u_i'}{\partial x_e}\right)^2 dV + \frac{\rho_p}{\rho}\frac{1}{\tau}(1-\mu_p)\bar{c}\int u_i'u_i' dV$$

$$+\frac{\rho_p}{\rho}\frac{1}{\tau}(1-c_2)c\bar{\mu}_p \int u_i' \frac{u_i'}{\bar{u}_i}\bar{u}_i dV \frac{\rho_p}{\rho}\frac{1}{\tau}(1-\mu_p)\mu_p^3\bar{c}$$

$$\times \int u_i'\left[-2\nu_T \frac{1}{2}\left(\frac{\partial(u_i'/u_1)}{\partial x_e} + \frac{\partial(u_e'/u_1)}{\partial x_i}\right)\right] dV$$

$$+g_i \frac{\rho_p}{\rho}\bar{c}\mu_p \int \frac{u_i'u_i'}{\bar{u}_1} dV. \quad (21)$$

To integrate the equation of fluctuational energy (21), it is necessary to prescribe the velocity profiles of the averaged and fluctuational flows of the carrying medium. The velocity profile of the averaged flow was prescribed by the power law

$$\bar{u}_+ = B(y_+)^m. \quad (22)$$

This yielded the expression for the coefficient of turbulent viscosity

$$\nu_T = \frac{\nu}{Bm}(y_+)^{1-m}. \quad (23)$$

The fluctuational velocities in macroscale vortices were prescribed by Townsend approximations [19]

$$u_1' = -u_2' = A\alpha^2 x_2 x_3 \exp\left[-(\tfrac{1}{2})\alpha^2(x_2^2+x_3^2)\right]$$

$$u_3' = A(1-\alpha^2 x_2^2)\exp\left[-(\tfrac{1}{2})\alpha^2(x_2^2+x_3^2)\right]. \quad (24)$$

After the substitution of equations (22), (23) and (24) into the fluctuational energy conservation equation (21) and integration of the latter with allowance for

$$1/\alpha = \delta_L, \quad (25)$$

the connection was obtained between the main characteristics of the flow

$$Bm(\delta_+)^{m+1}\Gamma\left(\frac{m+2}{2}\right) = \frac{(\delta_+)^{1-m}}{Bm}\left[\Gamma\left(\frac{2-m}{2}\right)(13-6m)\right.$$

$$-\Gamma\left(\frac{4-m}{2}\right)(19-8m)+\Gamma\left(\frac{6-m}{2}\right)(15-2m)$$

$$\left.-2\Gamma\left(\frac{8-m}{2}\right)\right]+\frac{15}{2}\sqrt{\pi}+(\delta_+)^2\frac{\nu}{u_*^2}\frac{\rho_p}{\rho}\frac{1}{\tau}\bar{c}$$

$$\times\left((1-\mu_p)\frac{5}{2}\sqrt{\pi}+(1-c_2)\mu_p\frac{\sqrt{\pi}}{2}\right)$$

$$-\frac{\rho_p}{\rho}\frac{1}{\tau}(1-\mu_p)\mu_p^3\bar{c}\frac{1}{mB^2}\frac{\nu}{u_*^2}(\delta_+)^{2-2m}$$

$$\times\left[\Gamma\left(\frac{3-2m}{2}\right)(4m-6)+\Gamma\left(\frac{5-2m}{2}\right)(8-2m)\right.$$

$$\left.-2m\Gamma\left(\frac{1-2m}{2}\right)-2\Gamma\left(\frac{7-2m}{2}\right)\right]$$

$$+\frac{\rho_p}{\rho}c\mu_p g_2 \frac{\nu}{u_*^3 B}(\delta_+)^{2-m}\Gamma\left(\frac{3-m}{2}\right). \quad (26)$$

The integral energy balance equation (26) was obtained for the horizontal orientation of the channel. In the case of a vertical ascending flow, the representation of the integral energy balance fully coincides with equation (26). In the case of an inclined orientation of the flow, the last term will include the

angle of channel inclination, whereas for the descending vertical flow the last term in equation (26) will change its sign and will account for the generation of turbulence rather than its dissipation. Consequently, the least advantageous flow regime is a vertically descending flow.

To simplify the representation of equation (26), the following designations were introduced

$$\Gamma_1(m) = m\Gamma\left(\frac{m+2}{2}\right) \tag{27}$$

$$\Gamma_2(m) = \Gamma\left(\frac{3-m}{2}\right) \tag{28}$$

$$\Gamma_3(m) = \frac{1}{m}\left[\Gamma\left(\frac{2-m}{2}\right)(13-6m) - \Gamma\left(\frac{4-m}{2}\right)(19-8m) + \Gamma\left(\frac{6-m}{2}\right)(15-2m) - 2\Gamma\left(\frac{8-m}{2}\right)\right] \tag{29}$$

$$\Gamma_4(m) = \frac{1}{m}\left[\Gamma\left(\frac{3-2m}{2}\right)(4m-6) + \Gamma\left(\frac{5-2m}{2}\right)(8-2m) - 2m\Gamma\left(\frac{1-2m}{2}\right) - 2\Gamma\left(\frac{7-2m}{2}\right)\right]. \tag{30}$$

With equations (27)–(30) taken into account, equation (26) can be transformed as

$$B(\delta_+)^{m+1}\Gamma_1(m) = \frac{(\delta_+)^{1-m}}{B}\Gamma_3(m) + \frac{15}{2}\sqrt{\pi} + (\delta_+)^2\frac{\nu}{u_*^2}\frac{\rho_p}{\rho}\frac{\bar{c}}{\tau}\left(\frac{5}{2}\sqrt{\pi}(1-\mu_p) + \frac{\sqrt{\pi}}{2}(1-c_2)\mu_p\right) - \frac{\rho_p}{\rho}\frac{\bar{c}}{\tau}(1-\mu_p)\mu_p^3\frac{1}{B^2}\frac{\nu}{u_*^2}(\delta_+)^{2-2m}\Gamma_4(m) + \frac{\rho_p}{\rho}\bar{c}\mu_p g_2\frac{\nu}{u_*^3 B}(\delta_+)^{2-m}\Gamma_2(m). \tag{31}$$

The integral energy balance equation (31) still has three unknown quantities: B, m, and δ_+. Consequently, to solve equation (31) it is necessary to additionally determine the connection between these parameters.

It is known that power profile of the averaged velocity satisfactorily describes experimental results only for the turbulent flow core. For the viscous sublayer, the linear law of velocity variation is valid. Within the scope of the adopted two-layer model of a turbulent boundary layer one has

$$\bar{u}_+ = y_+ \quad y_+ < \delta_+$$
$$\bar{u}_+ = B(y_+)^m \quad y_+ \geqslant \delta_+. \tag{32}$$

The condition for the equality of velocities should be fulfilled at the boundary of the viscous sublayer

$$y_+ = \delta_+ \quad \bar{u}_+ = \bar{u}_+. \tag{33}$$

Consequently

$$\delta_+ = B\delta_+^m \quad B = (\delta_+)^{1-m} \tag{34}$$

and equation (31) can be expressed as

$$(\delta_+)^2\left[\Gamma_1(m) - \frac{\nu}{u_*^2}\frac{\rho_p}{\rho}\frac{\bar{c}}{\tau}\left(\frac{5}{2}\sqrt{\pi}(1-\mu_p) + \frac{\sqrt{\pi}}{2}(1-c_2)\mu_p\right)\right] - (\delta_+)\frac{\rho_p}{\rho}c\bar{\mu}_p g_2\frac{\nu}{u_*^3}\Gamma_2(m) - \left(\Gamma_3(m) + \frac{15}{2}\sqrt{\pi} - \frac{\rho_p}{\rho}\frac{\bar{c}}{\tau}(1-\mu_p)\mu_p^3 \times \frac{\nu}{u_*^2}\Gamma_4(m)\right) = 0. \tag{35}$$

If the following conditions are fulfilled

$$\Gamma_1(m) > A\left(\frac{5}{2}\sqrt{\pi}(1-\mu_p) + \frac{\sqrt{\pi}}{2}(1-c_2)\mu_p\right) \tag{36}$$

or

$$A < \frac{\Gamma_1(m)}{\frac{5}{2}\sqrt{\pi}(1-\mu_p) + \frac{\sqrt{\pi}}{2}(1-c_2)\mu_p} \tag{37}$$

then equation (35) will have two real roots

$$\delta_+ = \frac{A\frac{\tau}{u_*}\mu_p g_2\Gamma_2(m) \pm \left\{\left(A - \frac{\tau}{u_*}\mu_p g_2\Gamma_2(m)\right)^2 + 4\left[\Gamma_1(m) - A\left(\frac{5}{2}\sqrt{\pi}(1-\mu_p) + \frac{\sqrt{\pi}}{2}(1-c_2)\mu_p\right)\right]\Gamma_3(m) + \frac{15}{2}\sqrt{\pi} - A(1-\mu_p)\mu_p^3\Gamma_4(m)\right\}^{1/2}}{2\left[\Gamma_1(m) - A\left(\frac{5}{2}\sqrt{\pi}(1-\mu_p) + \frac{\sqrt{\pi}}{2}(1-c_2)\mu_p\right)\right]} \tag{38}$$

where

$$A = \frac{\nu}{u_*^2}\frac{\rho_p}{\rho}\frac{\bar{c}}{\tau}. \tag{39}$$

Physically the quantity (δ_+) is real, therefore condition (36) for the existence of solution (38) must be considered as the restriction imposed on the region of applicability of the model as a whole.

To determine the sign in front of the square root in the numerator equation (38), zero concentration of

the dispersed phase in the flow was considered

$$\delta_+ = \pm\left(\frac{\Gamma_3(m)+\frac{15}{2}\sqrt{\pi}}{\Gamma_1(m)}\right)^{1/2}. \quad (40)$$

From this formula it follows that only the plus sign has a physical meaning.

The case of the zero concentration of the dispersed phase, equation (40), was also used to establish the relationship between the dimensionless viscous sublayer thickness δ_+ and the exponent m of the averaged velocity power profile, Fig. 3. From Fig. 3 it follows that to the interval of the possible values of the viscous sublayer thickness

$$5 \leqslant \delta_+ \leqslant 30 \quad (41)$$

there corresponds the range of the possible values of the exponent m

$$0.1 \leqslant m \leqslant 1. \quad (42)$$

The maximum agreement with the familiar experimental results (Fig. 4) and also with the generally adopted description of the averaged velocity profile by the logarithmic law of the wall and by the 1/7 and 1/10 power profiles are observed with the exponent $m = 0.348$. Moreover, this value of m determines the viscous sublayer thickness in a single-phase flow, $\delta_+ = 11.5$, which agrees perfectly with the original scheme of a turbulent boundary layer consisting of two strata. The values $m = 0.348$ and $\delta_+ = 11.5$ were therefore used in calculations when comparing the model proposed with experimental data.

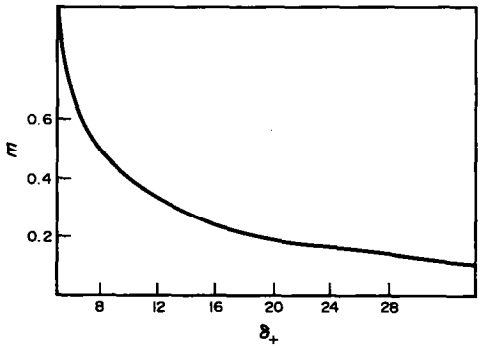

FIG. 3. Functional relationship between the viscous sublayer thickness and the exponent m.

The resulting relationship of the turbulent two-phase flow hydraulic resistance with the dispersed phase parameters was obtained from equations (1), (2), and (38). For this purpose, equations (1) and (2) were rewritten with the number 11.5 in equation (2) being replaced by the dimensionless single-phase flow viscous sublayer thickness

$$\lambda = \frac{8\tau_w}{\rho u_m^2} \quad u_*^2 = \left(\frac{\delta_{+1}\nu}{\delta_L}\right). \quad (43)$$

This allowed the determination of the relationship between the hydraulic resistance of turbulent two- and single-phase flows in the form

$$\frac{\lambda_2}{\lambda_1} = \frac{(\delta_{+1})^2}{(\delta_+)^2}. \quad (44)$$

With relations (38) and (40) taken into account, the resulting equation for the hydraulic resistance of a turbulent two-phase flow acquired the form

$$\frac{\lambda_2}{\lambda_1} = \frac{\left(\frac{\Gamma_3(m)+\frac{15}{2}\sqrt{\pi}}{\Gamma_1(m)}\right)\left\{2\left[\Gamma_1(m)-A\left(\frac{5}{2}\sqrt{\pi}(1-\mu_p)+\frac{\sqrt{\pi}}{2}(1-c_2)\mu_p\right)\right]\right\}^2}{A\frac{\tau}{u_*}\mu_p g_2\Gamma_2(m)+\left\{\left[\left(\Gamma_2(m)A\frac{\tau}{u_*}\mu_p g_2\right)^2+4(\Gamma_1(m)-A\left(\frac{5}{2}\sqrt{\pi}(1-\mu_p)+\frac{\sqrt{\pi}}{2}(1-c_2)\mu_p\right)\right](\Gamma_3(m)+\frac{15}{2}\sqrt{\pi}-A(1-\mu_p)\mu_p^3\Gamma_4(m))^2\right\}^{1/2}}. \quad (45)$$

Analysis of equation (45) showed that it correctly represents the approximation of the two-phase flow resistance to the single-phase turbulent friction when the dispersed phase concentration decreases to zero and describes the possible reduction of hydraulic losses in a dispersed phase-laden flow at certain concentrations of transferred particles.

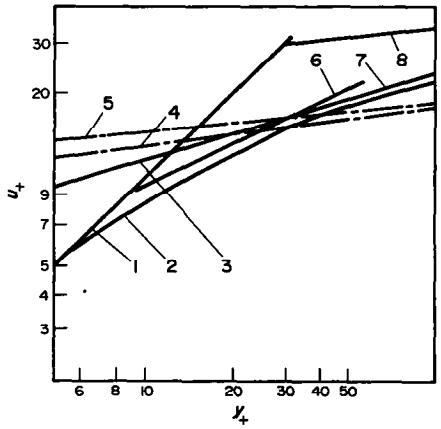

FIG. 4. Selection of the averaged velocity profile approximation for determining the viscous sublayer thickness. (1) $-\bar{u}_+ = y_+$, (2) $-\bar{u}_+ = 5\ln(y_+) - 3.05$, (3) $-\bar{u}_+ = 2.5\ln(y_+) + 5.5$, (4) $-\bar{u}_+ = 8.74(y_+)^{1/7}$, (5) $-\bar{u}_+ = 11.5(y_+)^{1/10}$, (6) $-\bar{u}_+ = B(y_+)^m$, $m = 1/2$, (7) $-\bar{u}_+ = B(y_+)^m$, $m = 0.348$, (8) $-\bar{u}_+ = B(y_+)^m$, $m = 1/8$.

The region of applicability of equation (45) is restricted, on the one hand, by conditions (36) and (37) for the existence of the solution to equation (35), and, on the other hand, by the fulfillment of complementary conditions that determine the minimum friction rate and the size of particles responsible for the turbulent flow 'laminarization' effect, The minimum possible dynamic velocity was obtained from the conditions of the existence of a two-phase flow [21]

$$\frac{1}{18}\frac{\rho_p}{\rho}\frac{d_p^2}{\nu} > \frac{\nu}{u_*^2} \quad \frac{1}{18}\frac{\rho_p}{\rho}\frac{d_p^2}{\nu} g < u_* \tag{46}$$

whence

$$u_{*_{min}} = (\nu g)^{1/3}. \tag{47}$$

When estimating the size of particles that allows the hydraulic resistance to be decreased, the Owen theory [22] was employed which assumes that the friction reduction is possible in a flow laden with particles the relaxation time of which is higher than the characteristic time of energy-containing vortices, but which does not exceed the characteristic time of the maximum possible vortices

$$0.1R < \tau u_* < R. \tag{48}$$

After the transition from the relaxation time to the diameter of particles with allowance for condition (47), the limits for the range of sizes were obtained with which the dispersed phase 'laminarizes' the turbulent flow

$$\left(1.8\frac{\rho}{\rho_p}\frac{\nu R}{u_*}\right)^{1/2} < d_p < \left(18\frac{\rho}{\rho_p}\frac{\nu R}{(\nu g)^{1/3}}\right)^{1/2}. \tag{49}$$

When constructing a relation for the maximum possible size of particles in horizontal systems, attention should be paid to the second equation of system (46). Here u_* is the specific dynamic velocity existing under the given conditions of the flow. The increase in the mean flow velocity leads to the growth of the dynamic velocity and, consequently, allows one to increase the size of the particles in the given case transported by the streams. On the other hand, the increase in the dynamic velocity according to equation (48) leads to a decrease in the 'lifetime' of energy-containing vortices and, consequently, in the size of the particles that allow one to obtain the reduction of friction. Since the aim of the present study is the determination of the limit for the 'laminarization' effect of the dispersed phase, it is evident that the latter trend will be dominating. By going over in equation (48) to the diameter of particles, the unknown relation was obtained in the form

$$d_p < \left(18\frac{\rho}{\rho_p}\frac{\nu P}{u_*}\right)^{1/2}. \tag{49}$$

Equation (45) gave the optimum dispersed phase concentration corresponding to the maximum decrease in friction with complete 'laminarization' of the flow when the drag of the turbulent two-phase flow is reduced to laminar friction

$$\frac{\rho_p}{\rho_{(\lambda_2=\lambda_1)}}\bar{c} = \frac{\tau u_*^2}{\nu} \frac{(\Gamma_3(m)+\frac{15}{2}\sqrt{\pi})(Re^{0.75}-202.275)}{\left(\frac{5}{2}\sqrt{\pi}(1-\mu_p)+\frac{\sqrt{\pi}}{2}(1-c_2)\mu_p\right)Re^{0.75}\dfrac{\Gamma_3(m)+\frac{15}{2}\sqrt{\pi}}{\Gamma_1(m)}} + \mu_p g_2 \Gamma_2(m)\frac{\tau}{u_*}\left(202.275R^{0.75}\frac{\Gamma_3(m)+\frac{15}{2}\sqrt{\pi}}{\Gamma_1(m)}\right)^{1/2} - 202.275(1-\mu_p)\mu_p^3\Gamma_4)(m) \tag{50}$$

Experimental investigations indicate, however, the unfeasibility of the effect of complete turbulent flow 'laminarization' by a dispersed phase, in view of which relation (50) may serve only as a qualitative estimate of the upper limit of concentration for the maximum decrease of losses in a turbulent two-phase flow.

4. COMPARISON OF PREDICTED RESULTS WITH EXPERIMENTAL DATA

In order to verify the proposed model, a comparison was carried out between the results predicted from the equations obtained and the available experimental data. The model demonstrates quite an identical decrease in the turbulent two-phase system drag for both a vertically ascending and a horizontal flow. This theoretical concept is confirmed by the experimental results of [10]—the sole source available at the disposal of the present authors which contains information about the influence of channel orientation in space on the value of hydraulic losses by a two-phase flow under other hydrodynamic conditions being equal. Figure 5 demonstrates a good coincidence of the results of calculation by equation (45) with the experiment considered.

An adequate representation of reality by the model suggested is also confirmed by Figs. 6 and 7 which contain the comparison of the predicted turbulent two-phase flow drag with the results of experiments [4, 14] for both horizontal and vertically ascending systems.

An analogous conclusion can also be drawn about the qualitative solution (50), since the behaviour of the relation for the optimum concentration, corresponding to the maximum reduction in friction,

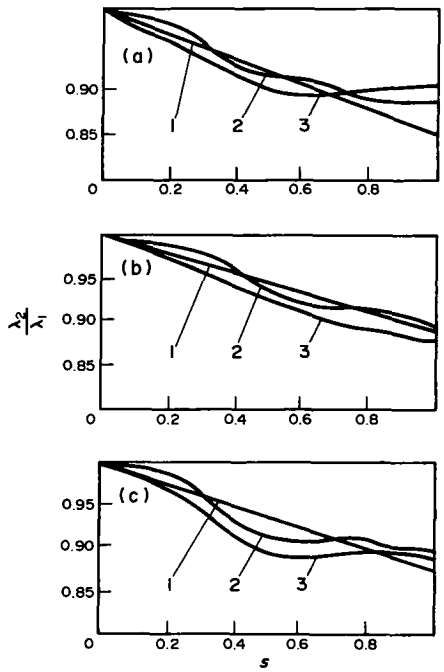

FIG. 5. Comparison of experimental and predicted results on the turbulent two-phase flow drag [10]. Air–glass particles: $D = 22.2$ mm, $\rho_p = 2500$ kg m^{-3}, $Re = 11\,000$. (1) Calculation from equation (45); (2) experiment in a horizontal tube; (3) experiment in a vertical tube. (a) $-d_p = 15$ μm, (b) $-d_p = 21$ μm, (c) $-d_p = 21.6$ μm.

coincides with the optimum concentration curve obtained experimentally in [15].

Concerning the critical dimensions of particles at which the friction effect begins to show up, then, according to the data of Fig. 2, the experimental values of the critical dimensions of particles are equal to 31, 28 and 165 μm, whereas the values calculated from equations (48) and (49) comprise 44, 42 and 160 μm, respectively. This allows a conclusion about a good agreement of prediction with experiment.

5. CONCLUSION

The proposed mathematical description of the dispersed phase effect on the turbulent carrying flow energy made it possible to generalize the reported fragmentary experimental data and to establish the general picture of the phenomenon and also to predict the friction reduction effect in a turbulent two-phase flow. Consequently, the proposed mathematical description allows the use of this effect in different branches of chemical technology and not only there.

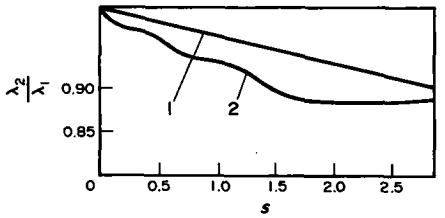

FIG. 6. Comparison of the experimental and predicted results on friction drag [4]. Air–corundum particles: horizontal channel with $D = 32.7$ mm, $\rho_p = 3970$ kg m^{-3}, $Re = 40\,000$, $d_p = 17$ μm, (1) calculation from equation (45), (2) experiment.

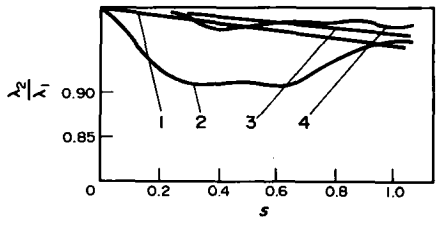

FIG. 7. Comparison of experimental and predicted results on friction drag [14]. Air–aluminium particles, vertical channel with $D = 50.,8$ mm, $\rho_p = 2700$ kg m^{-3}, $d_p = 15$ μm, $Re = 60\,000$, (1) calculation, (2) experiment, $Re = 76\,000$, (3) calculation, (4) experiment.

REFERENCES

1. M. Ye. Dogin and V. P. Lebedev, The effect of the size of particles on the resistance coefficient of a gas-suspension flow, *J. Engng Phys.* **2**, 26–30 (1959).
2. A. S. Mulgi, *Turbulent Two-phase Flows*, pp. 47–59. Institute of Thermal and Electrical Physics, Tallin (1979).
3. T. Jotaki and Y. Tomita, Solid velocities and pressure drops in a horizontal pneumatic conveying system, Pneumotransport 1, *2nd Int. Conf. on the Pneumatic Transport of Solids in Pipes*, B3-B15 (1971).
4. M. K. Laats, *Turbulent Two-phase Flows*, pp. 21–31. Institute of Thermal and Electrical Physics, Tallin (1979).
5. Yu. N. Pechenegov and V. G. Kashirskiy, *Turbulent Two-phase Flows*, pp. 84–90. Institute of Thermal and Electrical Physics, Tallin (1979).
6. B. I. Kosterin, L. Ye. Kostikov, V. A. Levchenko, V. V. Lozovetskiy and V. V. Perevezentsev, *Turbulent Two-phase Flows*, pp. 91–98. Institute of Thermal and Electrical Physics, Tallin (1979).
7. A. S. Mulgi, *Turbulent Two-phase Flows*, pp. 143–161. Institute of Thermal and Electrical Physics, Tallin (1976).
8. R. A. Duckwort and R. S. Kakka, The influence of particle size on the frictional pressure drops caused by the flow of a solid–gas suspension in a pipe, Pneumotransport 1, *2nd Int. Conf. on the Pneumatic Transport of Solids in Pipes*, pp. C3 (1971).
9. R. Pfefer and R. S. Kane, A review of drag reduction in dilute gas-solids suspensions in tubes, *Int. Conf. Drag Reduction*, p. F.1 (1974).
10. R. S. Kane, S. Weinbaum and R. Pfefer, Characteristics of dilute gas–solids suspensions in drag reducing flow, Pneumotransport 2, *2nd Int. Conf. on the Pneumatic Transport of Solids in Pipes*, pp. C3 (1973).
11. V. G. Kalmykov, Concerning the effect of suspended particles on the turbulent tube flow structure, *Zh. Prikl. Mekh. Tekh. Fiz.* No. 2, 111–118 (1976).
12. N. I. Gelperin, V. G. Ainshtein, L. I. Krupnik and Z. N. Mamedleyev, The hydraulic resistance of gas-suspension flows, *Izv. VUZov, Energetika* No. 2, 94–99 (1976).
13. R. G. Boothroyd and P. J. Walton, Fully developed turbulent boundary-layer flow of a fine solid particle gaseous suspension, *Ind. Engng Chem. Fundam.* **12**, 75–77 (1973).

14. B. S. Mason and R. G. Boothroyd, Comparison of friction factors in pneumatically conveyed suspensions using different sized particles in pipes of varying size, Pneumotransport 1, *2nd Int. Conf. on the Pneumatic Transport of Solids in Pipes*, pp. C3 (1973).
15. B. A. Askerov, Yu. A. Buyevich and Ya. M. Rasizade, About the change in the motion regimes and drag reduction on the introduction of particles into a viscous fluid flow, *Izv. Akad. Nauk SSSR, Mekh. Zhidk. Gaza* **4**, 80–83 (1968).
16. G. I. Barenblatt, Concerning the motion of suspended particles in a turbulent flow, *Prikl. Mat. Mekh.* **17**, 261–274 (1953).
17. Yu. A. Buyevich, Toward the model of drag reduction on the introduction of particles into a viscous fluid flow, *Izv. Akad. Nauk SSSR, Mekh. Zhidk. Gaza* **2**, 114–120 (1970).
18. L. V. Zakharov, A. A. Ovchinnikov and N. A. Nikolayev, The dispersed phase effect on the drag of a turbulent two-phase flow, *Teor. Osnovy Khim. Tekhn.* **22**, 647–654 (1988).
19. A. A. Townsend, *The Structure of Turbulent Shear Flow*. Cambridge University Press, Cambridge (1956).
20. Ye. P. Mednikov, *Turbulent Transfer and Deposition of Aerosols*. Nauka, Moscow (1981).
21. T. Jotaki and Y. Tomita, Turbulent friction drag of a dusty gas, Pneumotransport 1, *2nd Int. Conf. on the Pneumatic Transport of Solids in Pipes*, p. C5 (1971).
22. P. R. Owen, Pneumatic transport, *J. Fluid Mech.* **39**, (1969).